Electronic Supplementary Material (ESI) for Materials Chemistry Frontiers.

Supporting Information

Understanding Au Facet Effects in Photocatalytic Nonoxidative Coupling of Methane

Zhuo Liu, Biyang Xu, Xuanzhao Lu, Pan Li, Jun-Jie Zhu and Wenlei Zhu*

State Key Laboratory of Pollution Control and Resource Reuse, State Key Laboratory of Analytical Chemistry for Life Science, the Frontiers Science Center for Critical Earth Material Cycling, School of the Environment, School of Chemistry and Chemical Engineering, Nanjing University, Nanjing 210023, People's Republic of China

**E-mail: wenleizhu@nju.edu.cn*

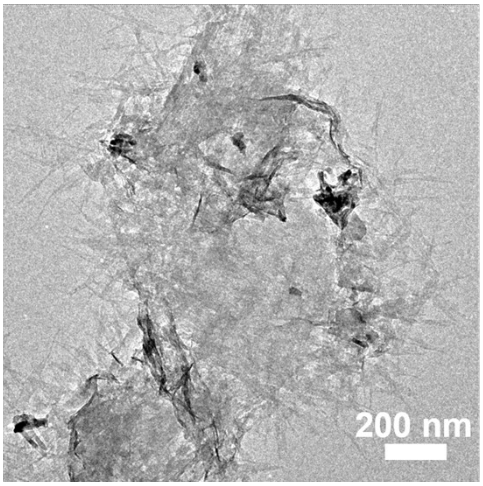

Figure S1. TEM images of ZnO nanosheets.

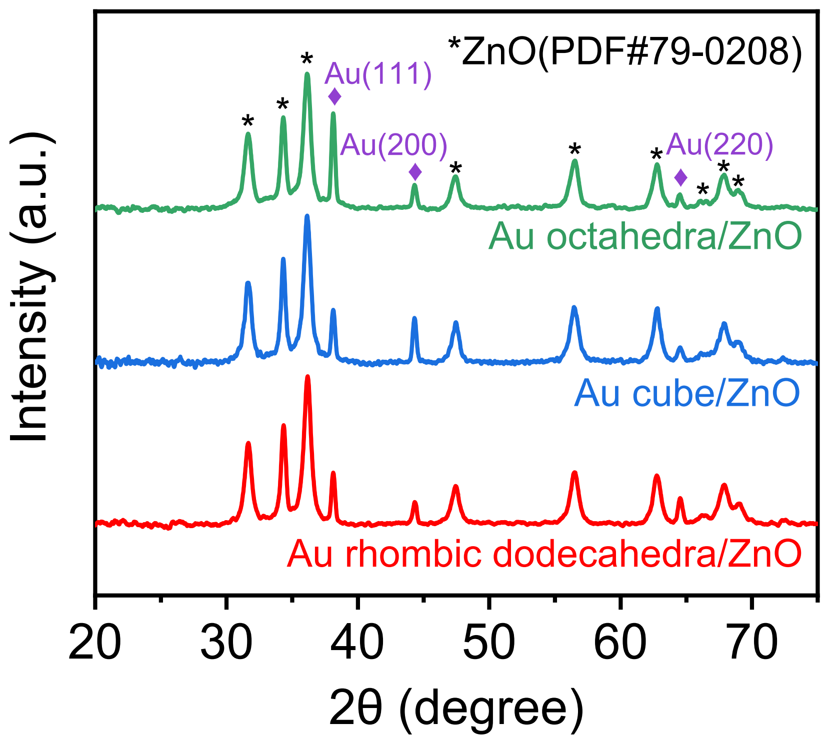

Figure S2. XRD patterns of Au/ZnO composite catalysts.

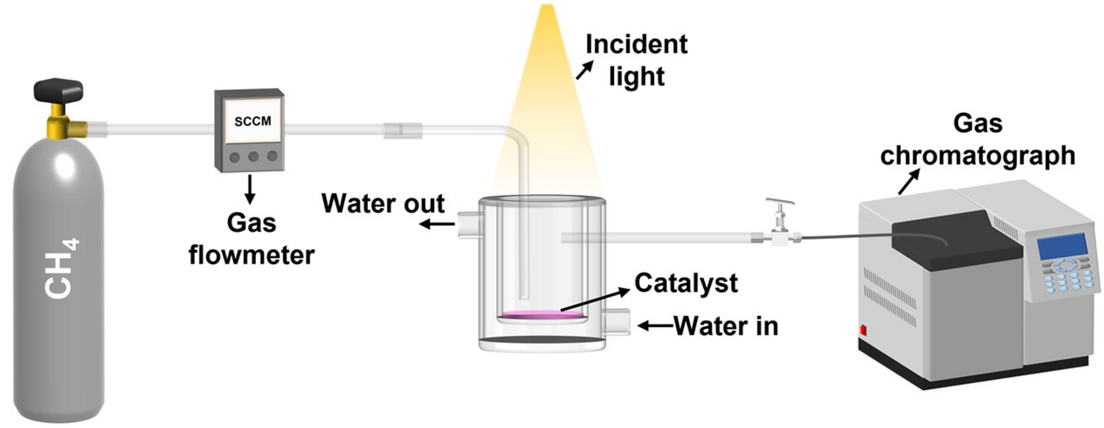

Figure S3. Schematic of the experimental set-up used to test photocatalytic NOCM reaction.

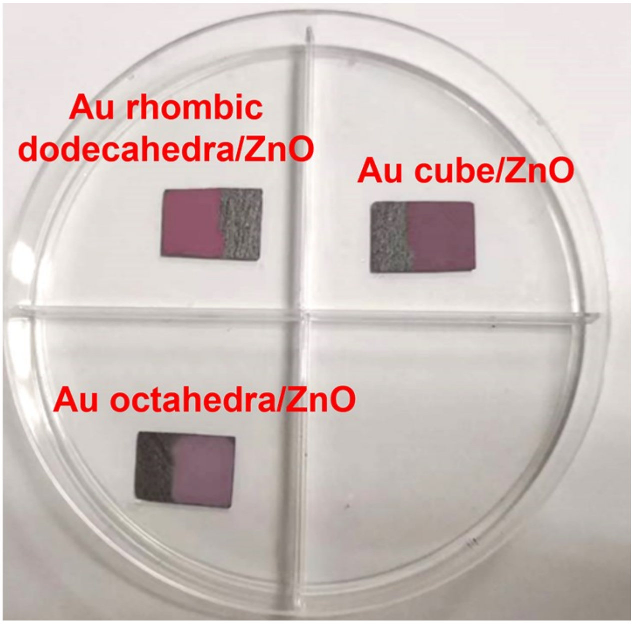

Figure S4. Schematic diagram of coating an equal amount of ZnO/Au hybrid catalysts on carbon paper.

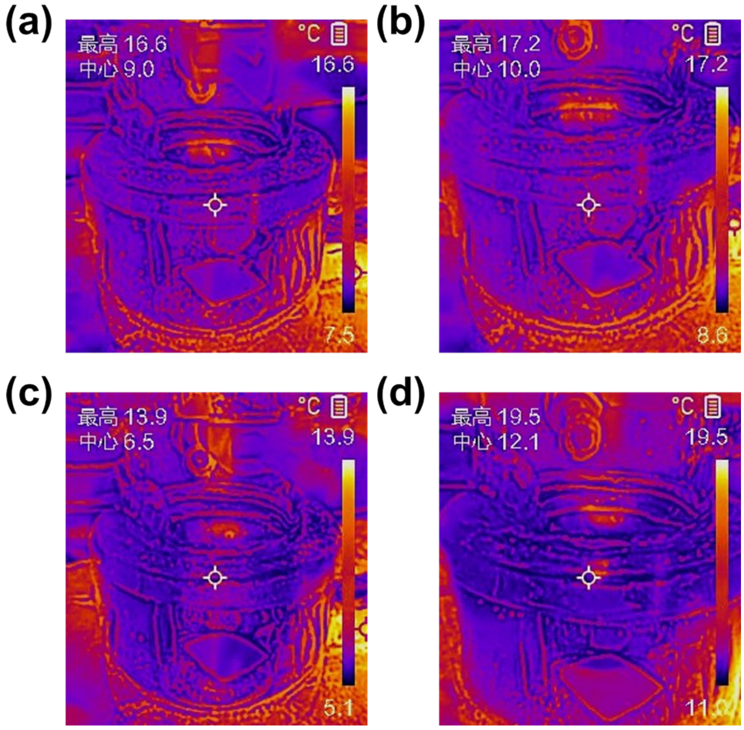

Figure S5. *In situ* thermographic photographs of Au octahedra/ZnO during catalytic reaction. (a) 0 h, (b) 1 h, (c) 2 h and (d) 3 h.

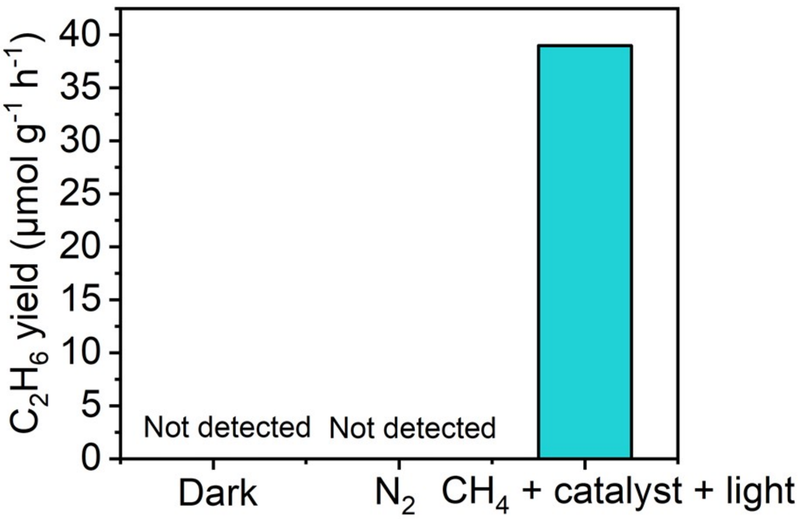

Figure S6. Performance of photocatalytic NOCM reaction under different conditions (the catalyst used is Au octahedra/ZnO hybrid catalyst).

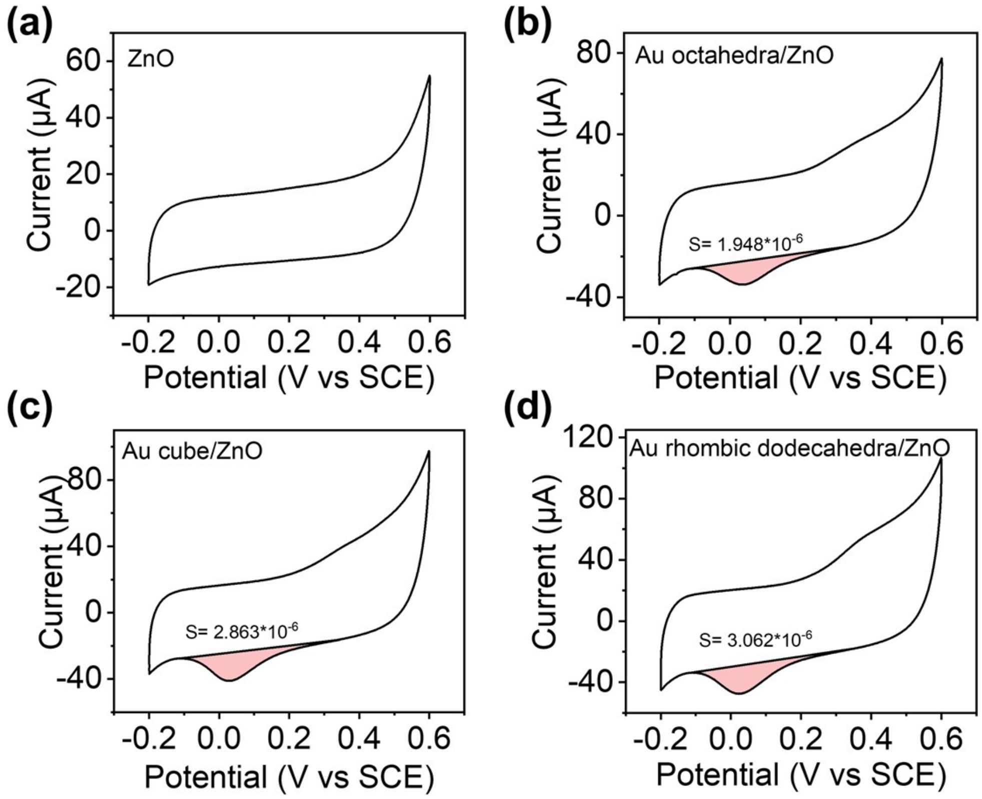

Figure S7. Cyclic voltammograms (CV) of Au/ZnO hybrid catalyst. (a) ZnO, (b) Au octahedra/ZnO, (c) Au cube/ZnO, (d) Au rhombic dodecahedra/ZnO. The electrolyte is 1 M NaOH and scan rate is 50 mV s^{-1}.

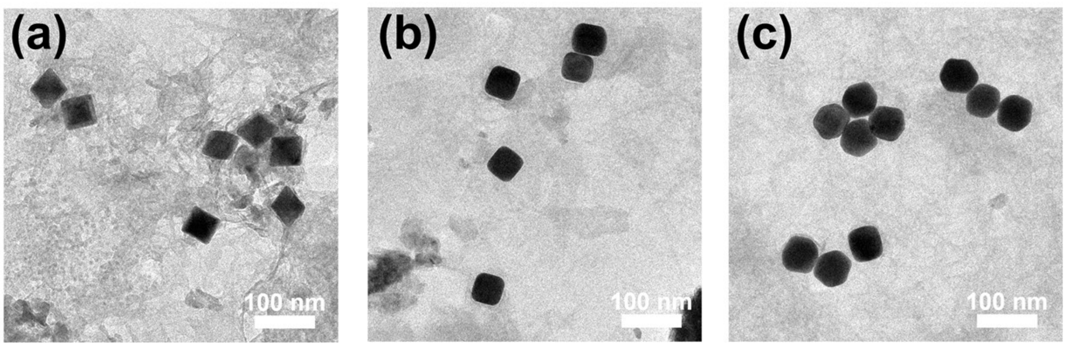

Figure S8. The morphology of Au/ZnO hybrid catalysts after 3 hours of reaction. (a) Au octahedra/ZnO. (b) Au cube/ZnO. (c) Au rhombic dodecahedra/ZnO.

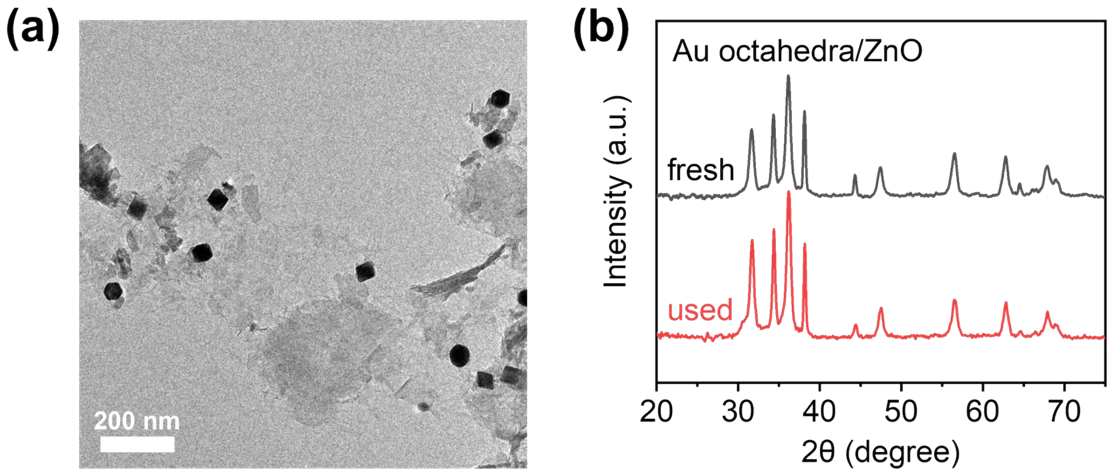

Figure S9. (a) The morphology of Au octahedra/ZnO hybrid catalyst after reaction. (b) XRD patterns of the fresh and used Au octahedra/ZnO photocatalyst.

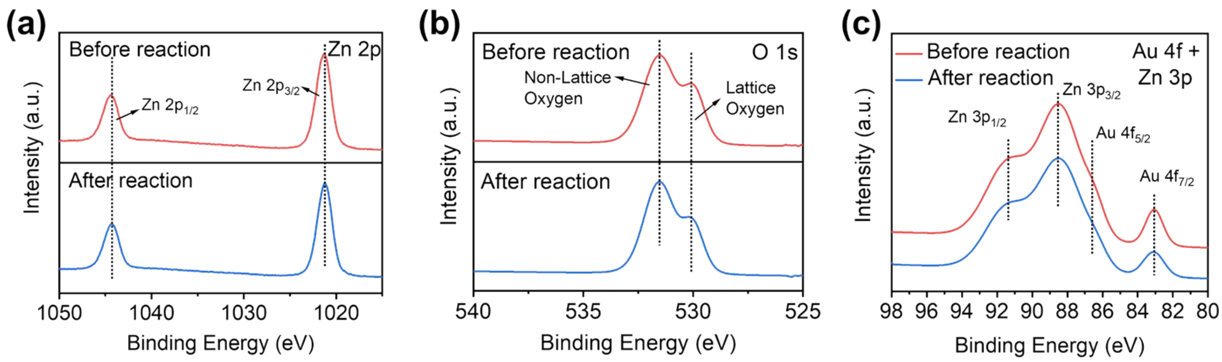

Figure S10. XPS spectra of the fresh and spent Au octahedra/ZnO photocatalyst. (a) Zn 2p, (b) O 1s and (c) Au 4f + Zn 3p spectra.

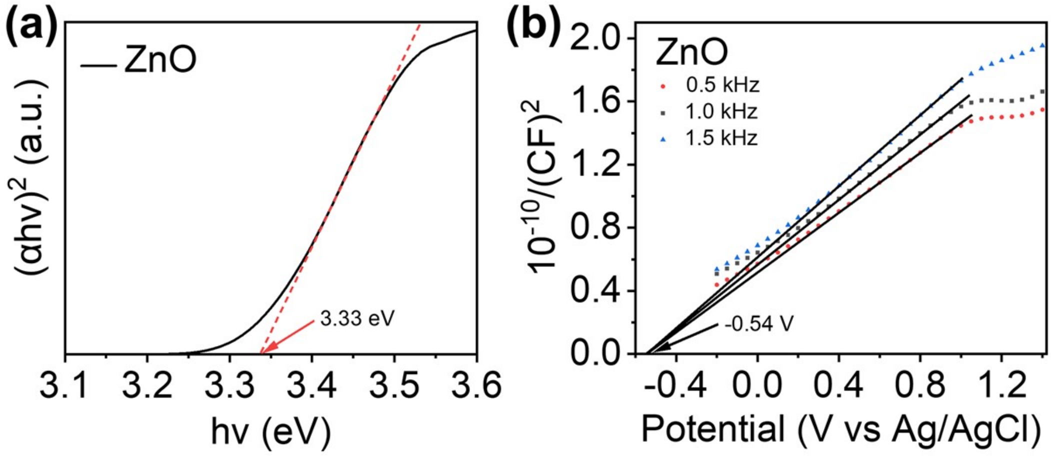

Figure S11. a) Tauc plots of ZnO nanosheets. b) Mott-Schottky curves of ZnO nanosheets. The flat band potential of ZnO can be obtained from Mott-Schottky measurements.

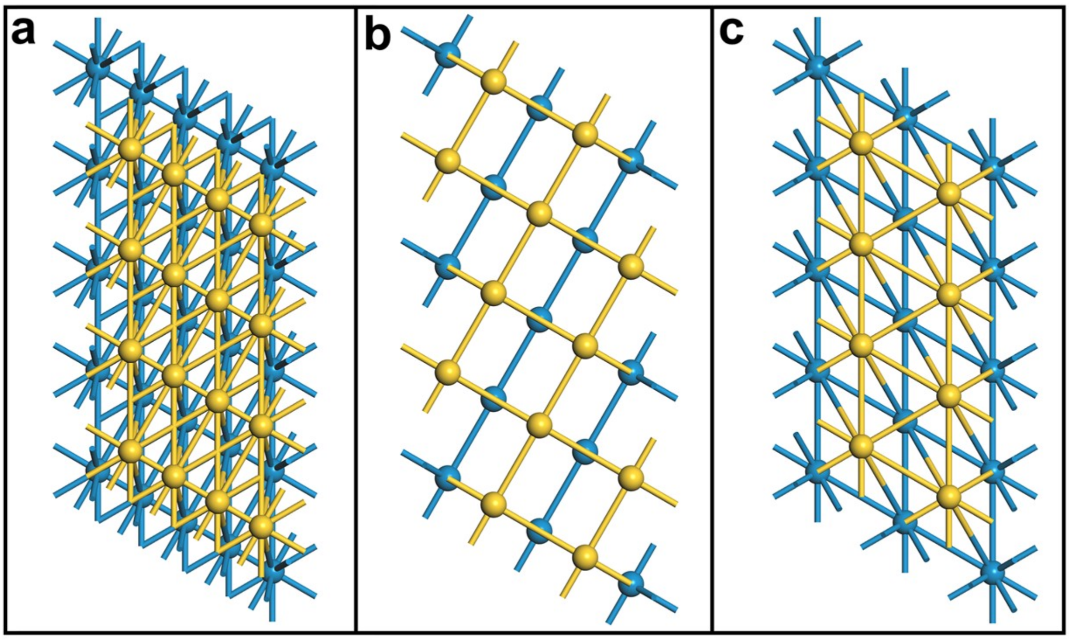

Figure S12. Model systems for a) Au(111), b) Au(100), c) Au(110).

Table S1. ICP-OES results of the final catalysts.

Catalysts	Content of Au (wt%)
Au octahedra/ZnO	2.81
Au cube/ZnO	2.88
Au rhombic dodecahedra/ZnO	2.89

Table S2. List of the values of the crystallographic orientation index (*N*) of Au octahedra/ZnO and Au cube/ZnO.

Catalysts	$N_{Au(111)}$	$N_{Au(100)}$	$N_{Au(110)}$
Au octahedra/ZnO	1.32	0.62	0.59
Au cube/ZnO	0.87	1.40	0.74

Table S3. The binding energy (BE) of Au 4f orbitals for all samples.

Samples	BE (Au $4f_{5/2}$)	BE (Au $4f_{7/2}$)
Au octahedra	87.9 eV	84.2 eV
Au cube	87.7 eV	84.0 eV
Au rhombic dodecahedra	87.7 eV	84.0 eV
Au octahedra/ZnO	86.4 eV	83.0 eV
Au cube/ZnO	86.6 eV	83.4 eV
Au rhombic dodecahedra/ZnO	86.6 eV	83.3 eV

Table S4. Representative works on photocatalytic NOCM reaction at room temperature and atmospheric pressure.

Catalyst	Conditions			Product (C_2H_6)	Reference
	Temperature	Light	Reactor		
Au(111)/ZnO Au(100)/ZnO Au(110)/ZnO	298 K	300 W Xe lamp (350 < λ < 780 nm)	Flow reactor	39.0 μmol g^{-1} h^{-1} 24.9 μmol g^{-1} h^{-1} 20.6 μmol g^{-1} h^{-1}	This work
(Zn^{+}, Zn^{2+})-ZSM-5	303 K	150 W high-pressure Hg lamp	Batch reactor	9.8 μmol g^{-1} h^{-1}	1
Ga^{3+}/EST-10	303 K	150 W high-pressure Hg lamp	Batch reactor	29.8 μmol g^{-1} h^{-1}	2
4.8 mol% Au/ZnO	Ambient temperature	300 W Xe lamp (320 < λ < 2500 nm), 600 mW cm^{-2}	Batch reactor	13.3 μmol g^{-1} h^{-1}	3
Pt/Ga-TiO_2-SiO_2	333 K	300 W Xe lamp	Batch reactor	1.57 μmol g^{-1} h^{-1}	4
Au/TiO_2(P25)	298 K	300 W Xe lamp (AM 1.5 G, 100 mW cm^{-2})	Flow reactor	81.74 μmol g^{-1} h^{-1}	5
Nb-TiO_2-SiO_2	Ambient temperature	300 W Xe lamp	Batch reactor	~2.0 μmol g^{-1} h^{-1}	6
GaN/ZnO	293 K	300 W Xe lamp (200 < λ < 400 nm)	Batch reactor	165 μmol g^{-1} h^{-1}	7
AuPd/ZnO	298 K	300 W Xe lamp	Batch reactor	36.7 μmol g^{-1} h^{-1}	8
Cu/Si-doped TiO_2	298 K	300 W Xe lamp	Flow reactor	33.8 μmol g^{-1} h^{-1}	9

Reference

1 L. Li, G.-D. Li, C. Yan, X.-Y. Mu, X.-L. Pan, X.-X. Zou, K.-X. Wang and J.-S. Chen, Efficient Sunlight-Driven Dehydrogenative Coupling of Methane to Ethane over a Zn^{+}-Modified Zeolite, *Angew. Chem. Int. Ed.*, 2011, **50**, 8299-8303.

2 L. Li, Y. Y. Cai, G. D. Li, X. Y. Mu, K. X. Wang and J. S. Chen, Synergistic effect on the photoactivation of the methane C-H bond over Ga^{3+}-modified ETS-10, *Angew. Chem. Int. Ed.*, 2012, **51**, 4702-4706.

3 L. Meng, Z. Chen, Z. Ma, S. He, Y. Hou, H.-H. Li, R. Yuan, X.-H. Huang, X. Wang, X. Wang and J. Long, Gold plasmon-induced photocatalytic dehydrogenative coupling of methane to ethane on polar oxide surfaces, *Energy Environ. Sci.*, 2018, **11**, 294-298.

4 S. Wu, X. Tan, J. Lei, H. Chen, L. Wang and J. Zhang, Ga-Doped and Pt-Loaded Porous TiO_2–SiO_2 for Photocatalytic Nonoxidative Coupling of Methane, *J. Am. Chem. Soc.*, 2019, **141**, 6592-6600.

5 J. Lang, Y. Ma, X. Wu, Y. Jiang and Y. H. Hu, Highly efficient light-driven methane coupling under ambient conditions based on an integrated design of a photocatalytic system, *Green Chem.*, 2020, **22**, 4669-4675.

6 Z. Chen, S. Wu, J. Ma, S. Mine, T. Toyao, M. Matsuoka, L. Wang and J. Zhang, Non-oxidative Coupling of Methane: N-type Doping of Niobium Single Atoms in TiO_2-SiO_2 Induces Electron Localization, *Angew. Chem. Int. Ed.*, 2021, **60**, 11901-11909.

7 G. Wang, X. Mu, J. Li, Q. Zhan, Y. Qian, X. Mu and L. Li, Light-Induced Nonoxidative Coupling of Methane Using Stable Solid Solutions, *Angew. Chem. Int. Ed.*, 2021, **60**, 20760-20764.

8 W. Jiang, J. Low, K. Mao, D. Duan, S. Chen, W. Liu, C.-W. Pao, J. Ma, S. Sang, C. Shu, X. Zhan, Z. Qi, H. Zhang, Z. Liu, X. Wu, R. Long, L. Song and Y. Xiong, Pd-Modified ZnO–Au Enabling Alkoxy Intermediates Formation and Dehydrogenation for Photocatalytic Conversion of Methane to Ethylene, *J. Am. Chem. Soc.*, 2021, **143**, 269-278.

9 J. Ma, J. Low, D. Wu, W. Gong, H. Liu, D. Liu, R. Long and Y. Xiong, Cu and Si co-doping on TiO_2 nanosheets to modulate reactive oxygen species for efficient photocatalytic methane conversion, *Nanoscale Horiz.*, 2022, **8**, 63-68.